

Article

# Synthesis, Crystal Structure and Thermal Stability of 1D Linear Silver(I) Coordination Polymers with 1,1,2,2-Tetra(pyrazol-1-yl)ethane

Evgeny Semitut<sup>1,2</sup>, Vladislav Komarov<sup>2,3</sup>, Taisiya Sukhikh<sup>2,3</sup>, Evgeny Filatov<sup>2,3</sup> and Andrei Potapov<sup>1,4,\*</sup>

<sup>1</sup> Department of Biotechnology and Organic Chemistry, National Research Tomsk Polytechnic University, 30 Lenin Ave., 634050 Tomsk, Russia; semitut@niic.nsc.ru

<sup>2</sup> Nikolaev Institute of Inorganic Chemistry, Siberian Branch of the Russian Academy of Sciences, Lavrentieva Ave., 3, 630090 Novosibirsk, Russia; komarov\_v\_y@ngs.ru (V.K.); sukhikh@niic.nsc.ru (T.S.); decan@niic.nsc.ru (E.F.)

<sup>3</sup> Department of Natural Sciences, Novosibirsk State University, Pirogova Str. 2, 630090 Novosibirsk, Russia

<sup>4</sup> Department of Chemical Engineering, Altai State Technical University, 46 Lenin Ave., 656038 Barnaul, Russia

\* Correspondence: potapov@tpu.ru; Tel.: +7-923-403-4103; Fax: +7-382-256-3865

Academic Editors: Thomas Doert and Mathias Wickleder

Received: 29 August 2016; Accepted: 21 October 2016; Published: 29 October 2016

**Abstract:** Two new linear silver(I) nitrate coordination polymers with bitopic ligand 1,1,2,2-tetra(pyrazol-1-yl)ethane were synthesized. Synthesized compounds were characterized by IR spectroscopy, elemental analysis, powder X-ray diffraction and thermal analysis. Silver coordination polymers demonstrated a yellow emission near 500 nm upon excitation at 360 nm. Crystal structures of coordination polymers were determined and structural peculiarities are discussed. In both of the structures, silver ions are connected via bridging ligand molecules to form polymeric chains with a five-atomic environment. The coordination environment of the central atom corresponds to a distorted trigonal bipyramid with two N atoms of different ligands in apical positions. The Ag–N bond distances vary in a wide range of 2.31–2.62 Å, giving strongly distorted metallacycles. Thermolysis of coordination polymers in reductive atmosphere (H<sub>2</sub>/He) leads to the formation of silver nanoparticles with a narrow size distribution.

**Keywords:** silver; coordination polymer; bitopic ligand; pyrazole; crystal structure; thermal analysis; luminescence; silver nanoparticles

## 1. Introduction

Silver is one of the metal ions most commonly used for the construction of coordination polymers owing to its wide range of coordination numbers (2 to 7 [1]) and its ability to comply with ligand geometry [2–5]. Silver coordination polymers are receiving much attention because of their antimicrobial [6–9], anti-tumor [10] and luminescent properties [11]. Bitopic bis- and tris(pyrazol-1-yl)methane ligands have been used for the preparation of coordination polymers of various topologies [12–20]. However, the simplest possible bitopic ligand, -1,1,2,2-tetra(pyrazol-1-yl)ethane (Pz<sup>4</sup>), has not been examined so far as a building block for silver coordination polymers. Recently, we have prepared this ligand and have demonstrated its ability to form both discrete complexes and coordination polymers with copper(II) ions [21,22]. Wang et al. reported the potential antibacterial and antifungal activity of the Pz<sup>4</sup> ligand [23]. Very recently, Dehury and coworkers reported the synthesis and crystal structure of catalytically active binuclear palladium(II) complexes with Pz<sup>4</sup> and similar ligands [24], but no silver coordination compounds with Pz<sup>4</sup> have been reported

so far. Herein we report the first synthesis and structural characterization of two new linear silver-Pz<sup>4</sup> coordination polymers.

## 2. Results and Discussion

### 2.1. Synthesis of Coordination Polymers

When the Pz<sup>4</sup> ligand (Figure 1) reacted with silver nitrate in ethanol or dimethylformamide (DMF) solutions, with coordination of the metal-to-ligand ratios close to 1:1, polymers **1** and **2** formed as polycrystalline powders. Recrystallization of the precipitates from DMF gave single crystals suitable for X-ray structure determination.

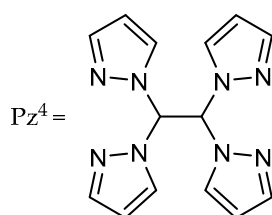


**Figure 1.** Bitopic 1,1,2,2-tetra(pyrazol-1-yl)ethane ligand (Pz<sup>4</sup>).

An attempt to carry out the reaction in solvothermal conditions at temperatures above 100 °C resulted in degradation of the Pz<sup>4</sup> ligand to smaller fragments (mostly pyrazole). This can be ascribed to the cleavage of C–C and C–N bonds catalyzed by Ag<sup>+</sup> ions in solution; similar processes have been observed before in other silver(I)–azole ligand systems [25]. When the metal-to-ligand ratio was increased, the same products were formed instead of binuclear complexes, while the excess of silver was precipitated as metal powder.

It is interesting to note that in contrast to many silver complexes, crystals of **1** and **2** are stable towards light and atmosphere and could be stored for several weeks without any precautions.

The coordination polymers **1** and **2** were characterized by IR spectroscopy, thermal analysis, single-crystal and powder X-ray diffraction methods.

The IR spectra of both compounds contain strong bands associated with ligands [26] and nitrate ion vibrations [27] (Figure S1). The patterns of the stretching and bending vibration bands of nitrate ions are somewhat different for compounds **1** and **2**, indicative of a slightly different nitrate coordination mode. Bands of indicative vibrations and geometric criteria for the nitrate ion coordination mode [28] are given in Table 1. Geometric criteria obtained from single-crystal diffraction data (see Section 2.2) indicate a unidentate coordination mode for both of the compounds, although for compound **1** the criteria ( $l_2-l_1$ ) and ( $A_1-A_2$ ) are close to boundary values of 0.6 Å and 28° [28]. Separation between the asymmetric stretching bands ( $\Delta\nu_3$ ) is also greater for this compound, suggesting a nitrate coordination mode intermediate between unidentate and anisobidentate.

**Table 1.** Bands of nitrate asymmetric stretching ( $\nu_3$ ) and in-plane bending ( $\nu_4$ ) vibrations and geometric coordination mode criteria.

Parameter	Compound 1	Compound 2
$\nu_3$ , cm <sup>-1</sup>	1390	1393
$\Delta\nu_3$ , cm <sup>-1</sup>	1294	1309
$\nu_4$ , cm <sup>-1</sup>	96	84
$l_2-l_1$ , Å <sup>1</sup>	770	755
$A_1-A_2$ , ° <sup>1</sup>	0.699	0.932
$l_3-l_2$ , Å <sup>1</sup>	33.49	47.72
	0.006	−0.085

<sup>1</sup>  $l_1 = d(\text{Ag-O1})$ ;  $l_2 = d(\text{Ag-O2})$ ;  $l_3 = d(\text{Ag-N1})$ ;  $A_1 = \theta(\text{Ag-O1-N1})$ ;  $A_2 = \theta(\text{Ag-O2-N1})$ .

## 2.2. Crystal Structures

According to the single-crystal XRD data, the complexes  $[\text{Ag}(\mu_2\text{-Pz}^4)(\text{NO}_3)]\text{DMF}_n$  (**1**) and  $[\{\text{Ag}(\mu_2\text{-Pz}^4)(\text{NO}_3)\}_n]$  (**2**) are polymeric and contain one  $\text{Ag}^+$  and  $\text{NO}_3^-$  units and two halves of the  $\text{Pz}^4$  ligands in the independent part expanded by the inversion center. Crystallographic data for compounds **1** and **2** are given in Table 2.

The crystal structure of **1** contains crystallization DMF molecules. In both of the crystal structures,  $\text{Ag}^+$  ions are connected via bridging ligand molecules in a chelating manner to form linear polymeric chains (Figure 2). The metal centers are surrounded by four nitrogen atoms of  $\text{Pz}^4$  and one oxygen atom of  $\text{NO}_3^-$  ions, giving a coordination number of five.

**Table 2.** Crystallographic data for compounds **1** and **2**.

Parameter	Compound 1	Compound 2
Empirical formula	$\text{C}_{17}\text{H}_{21}\text{AgN}_{10}\text{O}_4$	$\text{C}_{14}\text{H}_{14}\text{AgN}_9\text{O}_3$
Formula weight	537.31	464.21
Crystal system	Monoclinic	Triclinic
Space group	$P2_1/n$	$P-1$
Unit cell dimensions $a$ , Å	9.394(2)	7.8650(9)
$b$ , Å	14.299(4)	8.8031(10)
$c$ , Å	15.793(4)	13.2418(15)
$\alpha$ , °	90	74.380(4)
$\beta$ , °	94.173(7)	76.990(3)
$\gamma$ , °	90	83.647(4)
Volume, Å <sup>3</sup>	2115.7(9)	859.07(17)
Z	4	2
Density (calcd.), $\text{g}\cdot\text{cm}^{-3}$	1.687	1.795
$F(000)$	1088	464
Abs. coefficient, $\text{mm}^{-1}$	1.001	1.211
Crystal size, $\text{mm}^3$	$0.8 \times 0.15 \times 0.15$	$0.32 \times 0.08 \times 0.08$
$2\theta_{\text{max}}$ , °	51.38	53.58
Index range	$-11 \leq h \leq 11$ $-17 \leq k \leq 17$ $-19 \leq l \leq 11$	$-9 \leq h \leq 9$ $-10 \leq k \leq 8$ $-16 \leq l \leq 16$
Reflections collected	14199	7730
Independent reflections	3967 [R(int) = 0.0215]	3239 [R(int) = 0.0549]
Completeness to $2\theta = 51.38$ , %	98.7	99.4
Reflections, $I \geq 2\sigma(I)$	3786	2328
Parameters	291	250
Final R indices [ $I > 2\sigma(I)$ ]	R1 = 0.0665 wR2 = 0.1958	R1 = 0.0681 wR2 = 0.1577
R indices (all data)	R1 = 0.0679 wR2 = 0.1962	R1 = 0.0924 wR2 = 0.1771
GoF	1.277	1.037
Residual electron density (min/max, $e/\text{Å}^3$ )	-0.931/2.534	-2.227/1.646

In accordance with  $\tau_5$  criteria [29] (Table 3), the silver coordination environment corresponds to a distorted trigonal bipyramid with two nitrogen atoms of different ligands in apical positions. The Ag–N bond distances vary in a wide range of 2.31–2.62 Å, giving strongly distorted metallacycles (Table 4), which is typical for Ag complexes in the five-atomic environment [30–32]. The bond distances of  $\text{Pz}^4$  in the complexes are very close and are in accordance with those in known compounds with this ligand [21,22]. At the same time, there are deformation possibilities of the ligand due to the rotation of the heterocycles along the C1–N $m$  ( $m = 1, 2; n = 2, 4$ ) bond in different structures (Table 5). While the torsion angles C1–C1'–N $m$ –N $m$  in copper(II) complexes fall within the 61°–72° range, those in silver(I) compounds are lying in the range of 50°–58°, which is in accordance with the increased ionic

radius of  $\text{Ag}^+$  as compared with  $\text{Cu}^{2+}$ . The twisting mode of the ligand along the C1–C1' bond is permanent in all of the structures (the corresponding torsion angles Nmn–C1–C1'–Nmn fall within the  $55^\circ$ – $63^\circ$  range).

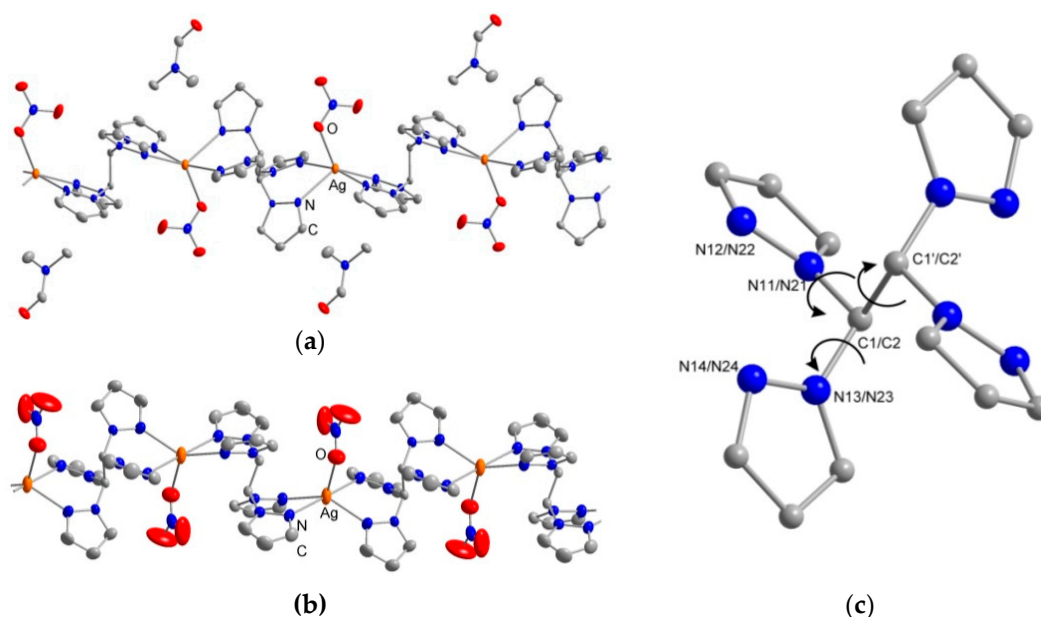


**Figure 2.** Thermal ellipsoid plots of complexes 1 (a) and 2 (b) showing 50% probability ellipsoids; (c) Atom numbering for compounds 1 and 2 and rotational modes of the Pz<sup>4</sup>. Hydrogen atoms have been omitted for clarity.

**Table 3.** Addison's  $\tau_5$  criteria for coordination centers in the complexes (1) and (2).

Parameter	$\{[\text{Ag}(\mu_2\text{-Pz}^4)(\text{NO}_3)]\text{DMF}\}_n$ (1)	$\{[\text{Ag}(\mu_2\text{-Pz}^4)(\text{NO}_3)]_n\}$ (2)
$\alpha$ ( $^\circ$ )	128.0	141.5
$\beta$ ( $^\circ$ )	166.8	178.0
$\tau_5 = (\beta - \alpha)/60$	0.64	0.61

**Table 4.** Selected bond distances ( $\text{\AA}$ ) for the complexes 1 and 2.

Parameter	$\{[\text{Ag}(\mu_2\text{-Pz}^4)(\text{NO}_3)]\text{DMF}\}_n$ (1)	$\{[\text{Ag}(\mu_2\text{-Pz}^4)(\text{NO}_3)]_n\}$ (2)
Ag–N12	2.41	2.30
Ag–N14	2.40	2.63
Ag–N22	2.54	2.49
Ag–N24	2.40	2.31
Ag–O1	2.58	2.60

**Table 5.** Torsion angles of ligand in copper(II) and silver(I) complexes with Pz<sup>4</sup> ligand.

Parameter	Nmn–C1–C1'–Nmn	C1–C1'–Nmn–Nmn
$\{[\text{Ag}(\mu_2\text{-Pz}^4)(\text{NO}_3)]\text{DMF}\}_n$ (1)	$\pm 55.5; \pm 54.8$	$\pm 57.9; \pm 53.8; \pm 50.4; \pm 54.8$
$\{[\text{Ag}(\mu_2\text{-Pz}^4)(\text{NO}_3)]_n\}$ (2)	$\pm 54.8; \pm 54.0$	$\pm 57.6; \pm 58.1; \pm 50.5; \pm 58.2$
$[\text{Cu}_2(\mu_2\text{-Pz}^4)(\text{H}_2\text{O})_2(\text{NO}_3)_4]$ [21]	$-58.9; 56.1; -57.3; 55.4$	$60.8; -70.4; 69.1; -61.7$ $70.4; -61.5; 63.2; -67.0$
$[\text{Cu}_2(\mu_2\text{-Pz}^4)(\text{H}_2\text{O})_6(\text{NO}_3)_4]$ [22]	$52.6; -61.7$	$59.5; -74.9; 67.7; -61.0$
$[\text{Cu}(\text{Pz}^4)(\text{NO}_3)_2]_n$ [22]	$\pm 56.0$	$\pm 72.2; \pm 61.5;$
$\{[\text{Cu}(\text{Pz}^4)(\text{H}_2\text{O})(\text{NO}_3)_2]_2\}_n$ [22]	$\pm 55.3$	$\pm 70.0; \pm 72.5$

Although the overall geometries of the chains of the complexes are alike, there are some quantitative differences. In **1**, the polymeric chain is less undulated than in **2**: deviations of silver atoms from their least square lines (the chain lines) are 0.53 Å and 1.18 Å, correspondingly (Figure 3). Nevertheless, the minimum Ag⋯Ag distances are close, being 7.15 and 7.09 Å, respectively. The position of NO<sub>3</sub><sup>−</sup> ions with respect to the chains is also different: in **1**, the angle between the chain line and the normal line of the {NO<sub>3</sub>} plane is 72.0° and that in (**2**) is 18.6°. The packing of chains in **1** imitates the hexagonal packing of cylinders with each chain surrounded by two translational equivalent ones in the *a* direction and four ones related to the 2<sub>1</sub> axes. The packing of chains in **2** is closer to the tetragonal one (Figure 4) with each chain surrounded by four translational-related ones.

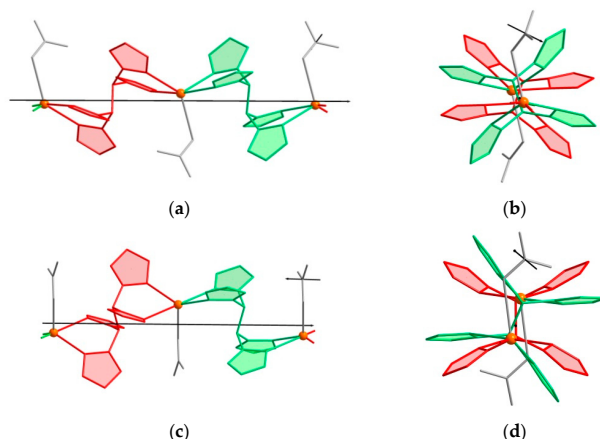


**Figure 3.** Fragments of the structures of **1** (a,b) and **2** (c,d). Black lines represent chain line through Ag<sup>+</sup> ions and normal lines of NO<sub>3</sub><sup>−</sup> ions planes.

The connectivity of the chains of the complexes **1** and **2** resembles that of known compound [Cu(Pz<sup>4</sup>)(NO<sub>3</sub>)<sub>2</sub>]<sub>n</sub> [21,22], with the exception of the additional coordinated NO<sub>3</sub><sup>−</sup> ligand. Despite this, their geometries are principally different in the mutual orientation of the neighboring ligands. Silver complexes are approximately related with mirror symmetry, resulting in a U-shaped chain form, whereas in the copper complex an approximate inversion and V-shape of the chain are observed [22]. Noticeably, the packing of chains in **1** is closer to [Cu((Pz<sup>4</sup>)(NO<sub>3</sub>)<sub>2</sub>)<sub>n</sub> rather than **2**.

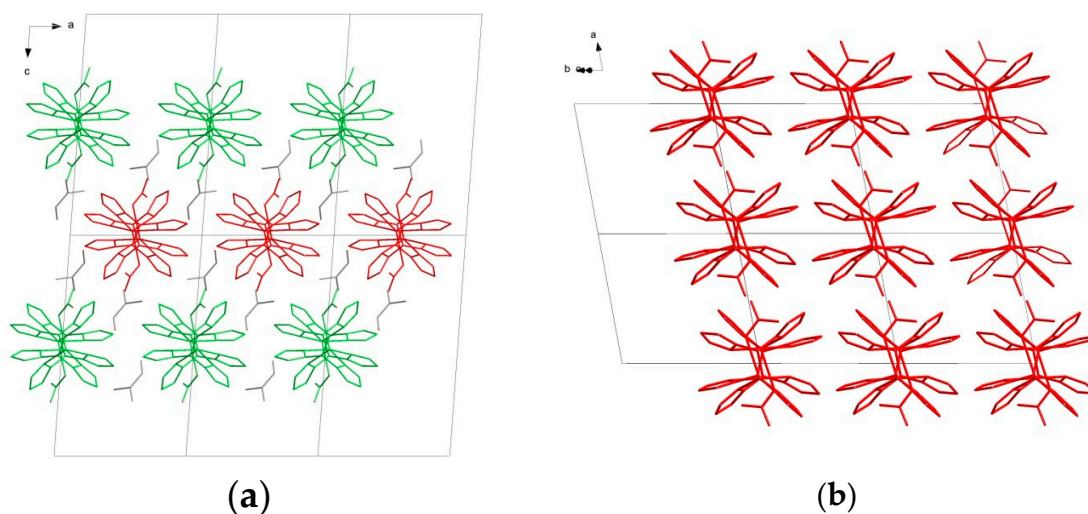


**Figure 4.** Packing patterns of the polymeric chains of the complexes **1** (a) and **2** (b).

### 2.3. Thermal and XRD Analyses

The thermal decomposition of complex **1** proceeds in two steps (Figure 5a). The first step is associated with the loss of solvate molecules that corresponds to 0.4 DMF molecules. The second step corresponds to the degradation of the polymer with the formation of silver nanoparticles and products of ligand destruction at 350 °C. Further thermolysis up to 800 °C leads to almost total destruction of these products, although silver nanoparticles still contain carbon traces. Thermal decomposition of **2** (Figure 5b) proceeds in one step, which is identical to the step of desolvated complex **1**. The only difference is the smaller size of the silver nanoparticles formed.

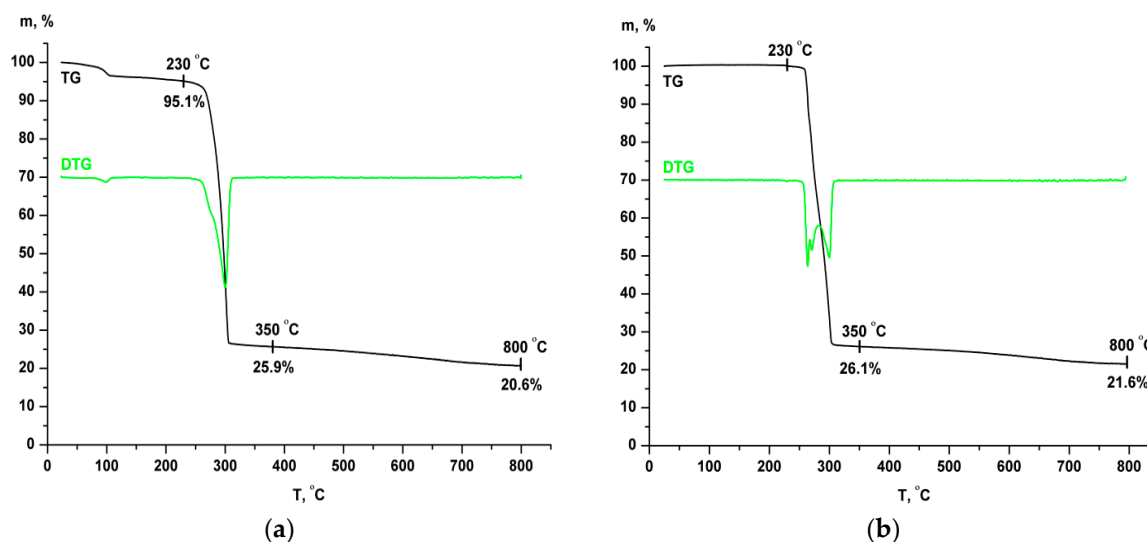


**Figure 5.** Curves of thermal analysis in inert atmosphere for complexes **1** (a) and **2** (b).

The influence of the atmosphere and final temperature of thermolysis on the crystallite size of the products has been studied for complex **2** (Table 6). Thermolysis of **2** in a reductive atmosphere has shown that parameters such as the annealing time and final temperature do not significantly influence the crystallite size of formed Ag nanoparticles, while in a helium atmosphere such dependence exists. TG curves in H<sub>2</sub>/He at 400 °C have shown that mass loss for **2** is a few percent lower than that calculated for compound **2** (Figure 6). It indicates that the formation of amorphous carbon occurs in a reductive atmosphere, which was confirmed by elemental analysis.

The formation of amorphous carbon obviously has a great influence on the stabilization of formed silver nanoparticles and its crystallite size was always in the range of 9–21 nm. On the other hand, the size distribution for nanoparticles formed in the helium atmosphere was wider and reached 12–53 nm (Table 6).

**Table 6.** Crystallite size of Ag nanoparticles: final products of  $[\{Ag(\mu_2\text{-Pz}^4)(\text{NO}_3)\}_n](2)$  thermolysis under different conditions.

Thermolysis Conditions (T, Annealing Time)	Crystallite Size Range for Different Atmospheres (nm)	
	He	H <sub>2</sub> /He (7.2%)
400 °C, 0 h	12–23	11–20
400 °C, 3 h	-	9–20
400 °C, 10 h	17–30	10–20
600 °C, 0 h	-	10–21
800 °C, 0 h	26–53	-

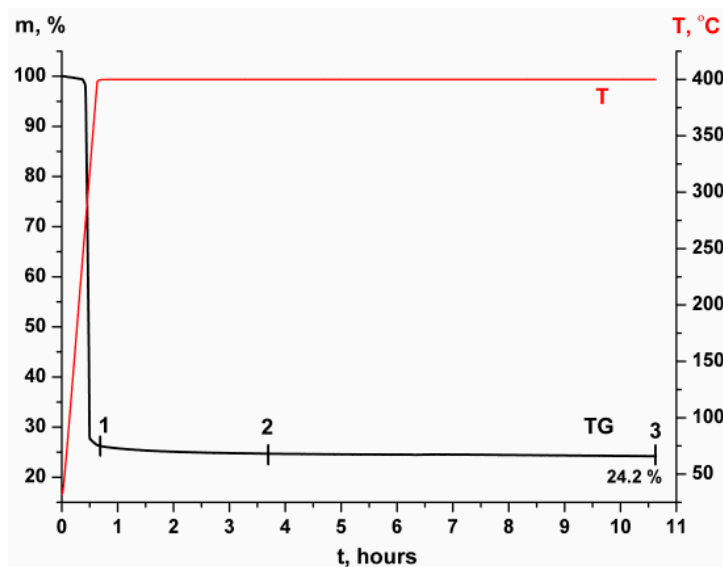


**Figure 6.** Curves of thermal analysis in reductive atmosphere (7.2% H<sub>2</sub>/He) for complex **2**. Points 1, 2 and 3 on the TG curve correspond to an annealing time of zero, three and ten hours.

The conformity of single crystals to synthesized bulk polycrystalline materials was established by comparison of experimental diffraction patterns with patterns calculated from single-crystal diffraction analysis data (Figure 7). The destruction of the polymer during 24 h synthesis was confirmed by XRD analysis.

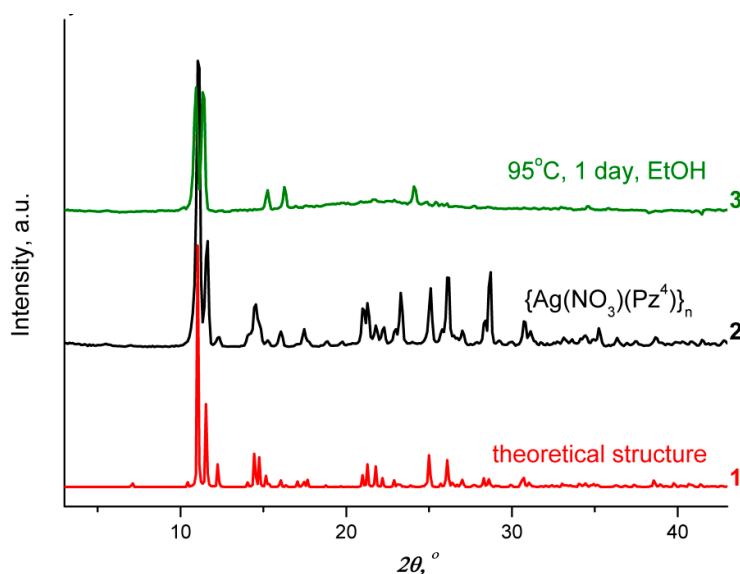


**Figure 7.** XRD patterns: (1) theoretical pattern of  $\{\text{Ag}(\text{NO}_3)(\mu_2\text{-Pz}^4)\}_n$  emulated from single-crystal experiment; (2) compound  $\{\text{Ag}(\text{NO}_3)(\mu_2\text{-Pz}^4)\}_n$ ; (3) products of  $\{\text{Ag}(\text{NO}_3)(\mu_2\text{-Pz}^4)\}_n$  degradation (solvothermal synthesis at ethanol solution during one day at 95 °C).

The XRD analyses of complex **1** and **2** conducted after several weeks have shown them to be stable under regular conditions.

#### 2.4. Solid-State Luminescence Studies

The emission properties of complex **2** were studied. In the solid state, the emission spectrum of **2** exhibits a broad band with a maximum at 500 nm, resulting in a yellow emission (Figure 8a).

The spectrum is independent of the excitation wavelength in the region of 300–430 nm. Within this region, the broad band is revealed in the excitation spectrum with a maximum at 360 nm (Figure 8b). The data obtained motivate in-depth investigation of the photophysical properties of the Pz<sup>4</sup> ligand and its transition metal complexes, which will be further carried out and reported separately.

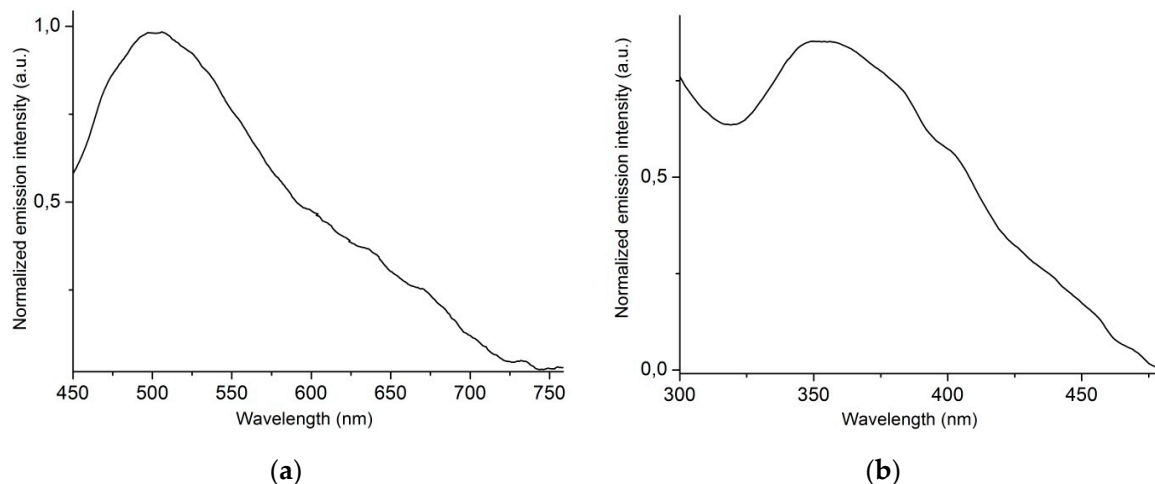


**Figure 8.** Emission spectrum of the complex **2** in solid state after excitation at 430 nm (a). Excitation spectrum at 500 nm emission wavelength (b).

### 3. Experimental Section

#### 3.1. Materials and Methods

The starting reagents used for synthesis of coordination compounds—AgNO<sub>3</sub> (chemical grade), dimethyl formamide (analytical grade), ethanol solution (95%, analytical grade) were used as received. Pz<sup>4</sup> ligand (1,1,2,2-tetra(pyrazol-1-yl)ethane) was prepared as reported previously [33]. Elemental analyses were carried out on Eurovector EuroEA 3000 analyzer (Eurovector SPA, Redavalle, Italy). Infrared (IR) spectra of solid samples as KBr pellets were recorded on a FT-801 spectrometer (4000–550 cm<sup>-1</sup>) (Kailas OU, Tallin, Estonia). Single crystals for crystal structure determination of **1** and **2** were mounted in inert oil and transferred to the diffractometer.

Single-crystal XRD data for **1** were collected by a X8Apex Bruker-Nonius diffractometer (Bruker Corporation, Billerica, MA, USA) equipped with a 4K CCD area detector at 150(2) K and for **2** were collected by a Bruker Apex DUO diffractometer equipped with a 4KCCD area detector at 298(2)K using the graphite-monochromated MoK $\alpha$  radiation ( $\lambda = 0.71073 \text{ \AA}$ ) (Bruker Corporation, Billerica, MA, USA). The  $\phi$ - and  $\omega$ -scan techniques were employed to measure intensities. Absorption corrections were applied with the use of the SADABS program [34]. The crystal structures were solved by direct methods and refined by full-matrix least squares techniques with the use of the SHELXTL package [35]. Atomic thermal displacement parameters for non-hydrogen atoms were refined anisotropically. The positions of hydrogen atoms were calculated corresponding to their geometrical conditions and refined using the riding model.

Polycrystalline samples were studied in  $2\theta$  range 5°–60° on a DRON RM4 powder diffractometer equipped with a CuK $\alpha$  source ( $\lambda = 1.5418 \text{ \AA}$ ) and graphite monochromator for the diffracted beam. Indexing of the diffraction patterns was done using data for compounds reported in the JCPDS-ICDD database [36] and WINFIT 1.2.1 [37] program, which allowed a calculation of the quantitative phase composition, the lattice parameters, and the crystallite size.

Thermal stability of coordination polymers was studied in inert (He) and oxidative (O<sub>2</sub>/Ar, 20%) atmospheres. Thermogravimetric measurements were carried out on a NETZSCH thermobalance TG 209 F1 Iris. Open Al<sub>2</sub>O<sub>3</sub> crucibles were used (loads 5–10 mg, heating rate 10 K·min<sup>-1</sup>).

Excitation and emission spectra of complex **2** in the solid state were recorded using Fluorolog-3 FL3-22 spectrophotometer (Horiba Jobin Yvon, Edison, NJ, USA). The spectra were corrected for the wavelength-dependent sensitivity of the detection.

### 3.2. Synthesis of Compounds

#### 3.2.1. Synthesis of $[\{Ag(\mu_2\text{-Pz}^4)(\text{NO}_3)\}_n\cdot\text{DMF}]_n$ (**1**)

A suspension of 29.4 mg  $\text{Pz}^4$  (0.1 mmol) in 5 mL of EtOH was added to 17.0 mg of  $\text{AgNO}_3$  (0.1 mmol) in glass vial. The mixture was stirred in the dark for 24 h at room temperature. During the first few hours of the synthesis initially undissolved needles of  $\text{Pz}^4$  disappear and colorless powder forms. The formed powder was then dissolved in 4 mL of DMF and left at room temperature in the dark. After three days colorless crystals formed at the bottom of the vial. They were filtered and washed twice with 4 mL of DMF and then dried on air for a few hours in the dark. The yield was 24.0 mg (45%). IR bands,  $\text{cm}^{-1}$ : 1520 (Pz), 1390, 1294 ( $\nu_3$ ), 1093 ( $\nu_1$ ), 1051 (Pz), 770 ( $\nu_4$ ). Elemental analysis: found, %: C 35.5, H 3.2, N 26.8; calculated ( $\text{AgC}_{14}\text{H}_{14}\text{N}_9\text{O}_3\cdot\text{DMF}$ ), %: C 38.0, H 3.9, N 26.1.

#### 3.2.2. Synthesis of $[\{Ag(\mu_2\text{-Pz}^4)(\text{NO}_3)\}_n]$ (**2**)

A suspension of 32.6 mg  $\text{Pz}^4$  (0.11 mmol) in 1 mL of DMF was added to 19.8 mg of  $\text{AgNO}_3$  (0.12 mmol) in glass vial. The mixture was stirred for 10 min at room temperature and then placed into an oven at 95 °C. After 8 h of heating the vial was allowed to cool to room temperature in the dark. After one day the crystals initially formed on the bottom increased in size. They were filtered and washed twice with 1 mL of DMF and then dried on air. The yield is 39.5 mg (77%). IR bands,  $\text{cm}^{-1}$ : 1521 (Pz), 1393, 1309 ( $\text{NO}_3$ ,  $\nu_3$ ), 1093 ( $\text{NO}_3$ ,  $\nu_1$ ), 1054 (Pz), 755 ( $\text{NO}_3$ ,  $\nu_4$ ). Elemental analysis: found, %: C 36.3, H 3.0, N 27.4; calculated ( $\text{AgC}_{14}\text{H}_{14}\text{N}_9\text{O}_3$ ), %: C 36.2, H 3.0, N 27.2.

## 4. Conclusions

In summary, synthesis and structural peculiarities of two new linear light- and air-stable silver- $\text{Pz}^4$  coordination polymers have been discussed. The investigation of the thermal properties of coordination polymers **1** and **2** revealed them to be stable up to 230 °C both in inert and oxidative atmospheres. The formation of silver nanoparticles with a narrow size distribution and the independence of particle size from thermolysis conditions demonstrate the possibility of using silver- $\text{Pz}^4$  coordination polymers for the generation of carbon-coated silver nanoparticles.

**Supplementary Materials:** The following are available online at <http://www.mdpi.com/2073-4352/6/11/138/s1>, Figure S1: IR spectra of coordination polymers **1** and **2**.

**Acknowledgments:** The reported study was supported by the Russian Science Foundation, Grant No. 15-13-10023.

**Author Contributions:** Evgeny Semitut and Andrei Potapov conceived and designed the experiments, Evgeny Semitut and Taisiya Sukhikh carried out the synthesis, Vladislav Komarov and Taisiya Sukhikh performed X-ray structure determination and analyzed the results, Evgeny Filatov performed X-ray powder diffraction analysis. All authors took part in the writing and discussion processes.

**Conflicts of Interest:** The authors declare no conflict of interest.

## Appendix A

Crystallographic data for the structural analysis have been deposited with the Cambridge Crystallographic Data Centre, CCDC No. 1499779 for compound **1** and 1499780 for compound **2**. Copies of the data can be obtained free of charge from the Cambridge Crystallographic Data Centre, 12 Union Road, Cambridge CB2 1EZ, UK (fax: +44-1223-336-033; e-mail:deposit@ccdc.cam.ac.uk).

## References

1. Beheshti, A.; Zafarian, H.R.; Khorramdin, R.; Fattahi Monavvar, M.; Abrahams, C.T. Novel silver(I) pyrazole-based coordination polymers: Synthetic and structural studies. *Polyhedron* **2012**, *48*, 245–252. [[CrossRef](#)]
2. Khlobystov, A.N.; Blake, A.J.; Champness, N.R.; Lemenovskii, D.A.; Majouga, A.G.; Zyk, N.V.; Schröder, M. Supramolecular design of one-dimensional coordination polymers based on silver(I) complexes of aromatic nitrogen-donor ligands. *Coord. Chem. Rev.* **2001**, *222*, 155–192. [[CrossRef](#)]
3. Bassanetti, I.; Atzeri, C.; Tinonin, D.A.; Marchiò, L. Silver(I) and Thioether-bis(pyrazolyl)methane Ligands: The Correlation between Ligand Functionalization and Coordination Polymer Architecture. *Cryst. Growth Des.* **2016**, *16*, 3543–3552. [[CrossRef](#)]
4. Avdeeva, V.V.; Malinina, E.A.; Sivaev, I.B.; Bregadze, V.I.; Kuznetsov, N.T. Silver and Copper Complexes with closo-Polyhedral Borane, Carborane and Metallacarborane Anions: Synthesis and X-ray Structure. *Crystals* **2016**, *6*, 60. [[CrossRef](#)]
5. Kirillov, A.M.; Wieczorek, S.W.; Lis, A.; Guedes da Silva, M.F.C.; Florek, M.; Król, J.; Staroniewicz, Z.; Smoleński, P.; Pombeiro, A.J.L. 1,3,5-Triaza-7-phosphaadamantane-7-oxide (PTA=O): New Diamondoid Building Block for Design of Three-Dimensional Metal–Organic Frameworks. *Cryst. Growth Des.* **2011**, *11*, 2711–2716. [[CrossRef](#)]
6. Jaros, S.W.; Guedes da Silva, M.F.C.; Florek, M.; Smoleński, P.; Pombeiro, A.J.L.; Kirillov, A.M. Silver(I) 1,3,5-Triaza-7-phosphaadamantane Coordination Polymers Driven by Substituted Glutarate and Malonate Building Blocks: Self-Assembly Synthesis, Structural Features, and Antimicrobial Properties. *Inorg. Chem.* **2016**, *55*, 5886–5894. [[CrossRef](#)] [[PubMed](#)]
7. Fromm, K.M. Silver coordination compounds with antimicrobial properties. *Appl. Organomet. Chem.* **2013**, *27*, 683–687. [[CrossRef](#)]
8. Jaros, S.W.; Guedes da Silva, M.F.C.; Król, J.; Conceição Oliveira, M.; Smoleński, P.; Pombeiro, A.J.L.; Kirillov, A.M. Bioactive Silver–Organic Networks Assembled from 1,3,5-Triaza-7-phosphaadamantane and Flexible Cyclohexanecarboxylate Blocks. *Inorg. Chem.* **2016**, *55*, 1486–1496. [[CrossRef](#)] [[PubMed](#)]
9. Jaros, S.W.; Smolenski, P.; da Silva, M.F.C.; Florek, M.; Krol, J.; Staroniewicz, Z.; Pombeiro, A.J.L.; Kirillov, A.M. New silver BioMOFs driven by 1,3,5-triaza-7-phosphaadamantane-7-sulfide (PTA=S): Synthesis, topological analysis and antimicrobial activity. *CrystEngComm* **2013**, *15*, 8060–8064. [[CrossRef](#)]
10. Smolenski, P.; Jaros, S.W.; Pettinari, C.; Lupidi, G.; Quassinti, L.; Bramucci, M.; Vitali, L.A.; Petrelli, D.; Kochel, A.; Kirillov, A.M. New water-soluble polypyridine silver(i) derivatives of 1,3,5-triaza-7-phosphaadamantane (PTA) with significant antimicrobial and antiproliferative activities. *Dalt. Trans.* **2013**, *42*, 6572–6581. [[CrossRef](#)] [[PubMed](#)]
11. Miao, S.-B.; Li, Z.-H.; Xu, C.-Y.; Ji, B.-M. Syntheses, characterization, and luminescence properties of three novel Ag(I) coordination polymers based on polycarboxylic acid ligands and 1,3-di-(1,2,4-triazole-4-yl)benzene. *CrystEngComm* **2016**, *18*, 4636–4642. [[CrossRef](#)]
12. Beheshti, A.; Zafarian, H.R.; Abrahams, C.T.; Bruno, G.; Rudbari, H.A. Investigating the effect of anion substitutions on the structure of silver-based coordination polymers. *Inorg. Chim. Acta* **2015**, *438*, 196–202. [[CrossRef](#)]
13. Gardinier, J.R.; Tatlock, H.M.; Hewage, J.S.; Lindeman, S.V. Cyclic versus Polymeric Supramolecular Architectures in Metal Complexes of Dinucleating Ligands: Silver(I) Trifluoromethanesulfonate Complexes of the Isomers of Bis(di(1H-pyrazolyl)methyl)-1,1'-biphenyl. *Cryst. Growth Des.* **2013**, *13*, 3864–3877. [[CrossRef](#)]
14. Reger, D.L.; Foley, E.A.; Smith, M.D. Synthesis of a tritopic, third-generation bis(1-pyrazolyl)methane ligand and its silver(I) complex: Unexpected structure with high coordination numbers. *Inorg. Chem. Commun.* **2010**, *13*, 568–572. [[CrossRef](#)]
15. Morin, T.J.; Merkel, A.; Lindeman, S.V.; Gardinier, J.R. Breaking the Cycle: Impact of Sterically-Tailored Tetra(pyrazolyl)lutidines on the Self-Assembly of Silver(I) Complexes. *Inorg. Chem.* **2010**, *49*, 7992–8002. [[CrossRef](#)] [[PubMed](#)]
16. Wang, S.; Zang, H.; Sun, C.; Xu, G.; Wang, X.; Shao, K.; Lan, Y.; Su, Z. Anion-directed genuine meso-helical supramolecular isomers of two 1D Ag(I) complexes based on arene-linked bis(pyrazolyl)methane ligands. *CrystEngComm* **2010**, *12*, 3458. [[CrossRef](#)]

17. Reger, D.L.; Watson, R.P.; Smith, M.D. Silver(I) complexes of fixed, polytopic bis(pyrazolyl)methane ligands: Influence of ligand geometry on the formation of discrete metallacycles and coordination polymers. *Inorg. Chem.* **2006**, *45*, 10077–10087. [[CrossRef](#)] [[PubMed](#)]
18. Reger, D.L.; Watson, R.P.; Gardinier, J.R.; Smith, M.D. Impact of Variations in Design of Flexible Bitopic Bis(pyrazolyl)methane Ligands and Counterions on the Structures of Silver(I) Complexes: Dominance of Cyclic Dimeric Architecture. *Inorg. Chem.* **2004**, *43*, 6609–6619. [[CrossRef](#)] [[PubMed](#)]
19. Reger, D.L.; Gardinier, J.R.; Christian Grattan, T.; Smith, M.R.; Smith, M.D. Synthesis of the silver(I) complex of  $\text{CH}_2[\text{CH}(\text{pz}^{4\text{Et}})_2]_2$  containing the unprecedented  $[\text{Ag}(\text{NO}_3)_4]^{3-}$  anion: A general method for the preparation of 4-(alkyl)pyrazoles. *New J. Chem.* **2003**, *27*, 1670–1677. [[CrossRef](#)]
20. Reger, D.L.; Semeniuc, R.F.; Silaghi-Dumitrescu, I.; Smith, M.D. Influences of Changes in Multitopic Tris(pyrazolyl)methane Ligand Topology on Silver(I) Supramolecular Structures. *Inorg. Chem.* **2003**, *42*, 3751–3764. [[CrossRef](#)] [[PubMed](#)]
21. Potapov, A.S.; Nudnova, E.A.; Khlebnikov, A.I.; Ogorodnikov, V.D.; Petrenko, T.V. Synthesis, crystal structure and electrocatalytic activity of discrete and polymeric copper(II) complexes with bitopic bis(pyrazol-1-yl)methane ligands. *Inorg. Chem. Commun.* **2015**, *53*, 72–75. [[CrossRef](#)]
22. Semitut, E.Y.; Komarov, V.Y.; Filatov, E.Y.; Kuznetsova, A.S.; Khlebnikov, A.I.; Potapov, A.S. Synthesis and structural characterization of copper(II) coordination polymers with 1,1,2,2-tetra(pyrazol-1-yl)ethane. *Inorg. Chem. Commun.* **2016**, *64*, 23–26. [[CrossRef](#)]
23. Wang, J.-X.; Zhu, Z.-R.; Bai, F.-Y.; Wang, X.-Y.; Zhang, X.-X.; Xing, Y.-H. Molecular design and the optimum synthetic route of the compounds with multi-pyrazole and its derivatives and the potential application in antibacterial agents. *Polyhedron* **2015**, *99*, 59–70. [[CrossRef](#)]
24. Dehury, N.; Maity, N.; Tripathy, S.K.; Basset, J.-M.; Patra, S. Dinuclear Tetrapyrazolyl Palladium Complexes Exhibiting Facile Tandem Transfer Hydrogenation/Suzuki Coupling Reaction of Fluoroarylketone. *ACS Catal.* **2016**, *6*, 5535–5540. [[CrossRef](#)]
25. Heath, R.; Muller-Bunz, H.; Albrecht, M. Silver(I) NHC mediated C-C bond activation of alkyl nitriles and catalytic efficiency in oxazoline synthesis. *Chem. Commun.* **2015**, *51*, 8699–8701. [[CrossRef](#)] [[PubMed](#)]
26. Nudnova, E.A.; Potapov, A.S.; Khlebnikov, A.I.; Ogorodnikov, V.D. Synthesis of ditopic ligands containing bis(1H-pyrazol-1-yl)-methane fragments. *Russ. J. Org. Chem.* **2007**, *43*, 1698–1702. [[CrossRef](#)]
27. Nakamoto, K. *Infrared and Raman Spectra of Inorganic and Coordination Compounds, Part B. Applications in Coordination, Organometallic, and Bioinorganic Chemistry*; Wiley-Interscience: Hoboken, NJ, USA, 2009.
28. Kleywegt, G.J.; Wiesmeijer, W.G.R.; Van Driel, G.J.; Driessen, W.L.; Reedijk, J.; Noordik, J.H. Unidentate versus symmetrically and unsymmetrically bidentate nitrate co-ordination in pyrazole-containing chelates. The crystal and molecular structures of (nitrate-O)[tris(3, 5-dimethylpyrazol-1-ylmethyl) amine] copper (II) nitrate, (nitrate-O, O')[tris(3, 5-dimethylpyrazol-1-ylmethyl) amine] nickel (II) nitrate, and (nitrate-O)(nitrate-O, O')[tris(3, 5-dimethylpyrazol-1-ylmethyl) amine] cadmium (II). *J. Chem. Soc. Dalt. Trans.* **1985**, 2177–2184. [[CrossRef](#)]
29. Addison, A.W.; Rao, T.N.; Reedijk, J.; van Rijn, J.; Verschoor, G.C. Synthesis, structure, and spectroscopic properties of copper(II) compounds containing nitrogen-sulphur donor ligands; the crystal and molecular structure of aqua[1,7-bis(N-methylbenzimidazol-2'-yl)-2,6-dithiaheptane]copper(II) perchlorate. *J. Chem. Soc. Dalt. Trans.* **1984**, 1349–1356. [[CrossRef](#)]
30. Zhang, R.; Zhao, J.; Xi, X.; Yang, P.; Shi, Q. A Novel Silver(I) Complex with 4,5-Diazafluoren-9-one and the Interaction Study Between the Complex and DNA. *J. Chem. Crystallogr.* **2011**, *41*, 209–213. [[CrossRef](#)]
31. Marandi, F.; Hosseini, N.; Krautscheid, H.; Lässig, D.; Lincke, J.; Rafiee, M.; Asl, Y.A. Synthesis and structural characterization of new dinuclear silver(I) complexes: Different coordination modes of substituted 1,2,4-triazine ligands. *J. Mol. Struct.* **2011**, *1006*, 324–329. [[CrossRef](#)]
32. Zhang, F.; Yang, Y.-L. (Nitrate-κO)bis[5-(pyridin-2-yl)pyrazine-2-carbonitrile-κ<sup>2</sup>N<sub>4</sub>,N<sub>5</sub>]silver(I). *Acta Crystallogr. Sect. E* **2011**, *67*, m1863. [[CrossRef](#)] [[PubMed](#)]
33. Potapov, A.S.; Nudnova, E.A.; Khlebnikov, A.I.; Ogorodnikov, V.D.; Petrenko, T.V. Synthesis of new polydentate pyrazolyl-ethene ligands by interaction of 1H-pyrazole and 1,1,2,2-tetrabromoethane in a superbasic medium. *J. Heterocycl. Chem.* **2011**, *48*, 645–651. [[CrossRef](#)]

34. Bruker. *APEX2 (Version 2.0), SAINT (Version 8.18c), and SADABS (Version 2.11)*; Bruker Advanced X-ray Solutions, Bruker AXS Inc.: Madison, WI, USA, 2000–2012.
35. Sheldrick, G.M. A short history of SHELX. *Acta Cryst.* **2008**, *A64*, 112–122. [[CrossRef](#)] [[PubMed](#)]
36. *PCPDFWIN. v. 1.30*; JCPDS-ICDD: Swarthmore, PA, USA, 1997.
37. Krumm, S. An Interactive Windows Program for Profile Fitting and Size/Strain Analysis. *Mater. Sci. Forum* **1996**, *228–231*, 183–190. [[CrossRef](#)]



© 2016 by the authors; licensee MDPI, Basel, Switzerland. This article is an open access article distributed under the terms and conditions of the Creative Commons Attribution (CC-BY) license (<http://creativecommons.org/licenses/by/4.0/>).